Int. J. Electrochem. Sci., 14 **(2019)** 5646 – 5653, doi: 10.20964/2019.06.03

International Journal of
ELECTROCHEMICAL
SCIENCE
www.electrochemsci.org

Short Communication

Sonoelectrochemical Synthesis of Nanostructured of p-Cu_2O and n-Fe_2O_3 and Their Application for Photoelectrochemical Splitting of Water

P. Grez[1,], R. Henríquez[1], E. Muñoz[1], C. Rojas[1], S. Moreno[1], G. Sessarego[1], C. Heyser[1], C. Celedón[2], and R. Schrebler[1]*

[1]Instituto de Química, Pontificia Universidad Católica de Valparaíso, Avda. Universidad 330, Curauma, Placilla,
Valparaíso Casilla, 4059 Valparaíso, Chile
[2] Departamento de Física, Universidad Técnica Federico Santa María, P.O. Box 110-V, Valparaíso, Chile
[*]E-mail: paula.grez@pucv.cl

Received: 20 June 2018 / *Accepted:* 29 January 2019 / *Published:* 10 May 2019

In the present work, a p-Cu_2O nanostructured electrode and n-Fe_2O_3 nanotubes electrode, were used as photocathode and photoanode, respectively, for study the splitting of water. In this photoelectrochemical cell (PEC) the oxygen evolution reaction takes place in the photoanode and the hydrogen evolution reaction in the photocathode, both from the water decomposition reaction. In this case, the two electrodes were synthesized by ultrasound-assisted anodization (37 kHz, 60 W) in corresponding sheet metallic. The experimental conditions for the formation of p-Cu_2O nanostructures were: 75 V, 75°C and 900 s of polarization in a solution of ethylene glycol with 5% wt of water and 0.5% wt of NH_4Cl [1]. On the other hand, the Fe_2O_3 nanotubes were synthesized at 50 V, 50°C and 180 s of polarization in an ethylene glycol solution containing 3% wt of water and 0.5% wt of NH_4F [2]. In both cases, after the anodization, the sheets were thermally treated at 190°C for 90 min in an argon atmosphere for p-Cu_2O and for n-Fe_2O_3 at 500°C for 180 min in an oxygen atmosphere. Subsequently, the electrodes were characterized by DRS, EIE by Mott-Schottky plots obtaining the diagrams of respective bands. Finally, electrochemical measurements were performed with the system Fe|nanotubes n-Fe_2O_3|0.1 M Na_2SO_4 (pH 10)|p-Cu_2O nanostructured|Cu, where the two electrodes were illuminated. In this context, the system required a bias potential of 0.36 V. This value corresponds to 69.5 kJ/mol, for a current density of 0.3 $mAcm^{-2}$. On the other hand, in equal conditions of current density, but using platinum electrodes, a bias potential of 1.50 V (289.5 kJ/mol) was required. In this context, a decrease in the energy cost for the decomposition reaction of water, in an alkaline solution was evidenced.

Keywords: sonoelectrochemical synthesis, nanostrutured copper oxides, nanostructured Fe_2O_3, photoelectrochemical cell.

1. INTRODUCTION

The solar energy that reaches the earth's surface is greater than the energy that humanity currently needs. Therefore, in the future and taking into account the growth of the world population, this amount of energy could easily satisfy the required consumption. However, low cost devices are required that efficiently transform solar energy into useful energies or non-polluting fuels. An example are the photoelectrochemical cells (PEC), devices employed for the conversion of solar energy into chemical energy, eg., Hydrogen generation from the splitting of water. Currently, it is expected that this type of device is made up of semiconductor (SC) electrodes. Among the promising materials for the manufacture of photoelectrodes, appears for the copper (I) oxide, which is an intrinsic p-type semiconductor with a band gap value of ~2.0 eV [1,3-5] and iron (III) oxide what is a n-type semiconductor and also has a band gap value of ~2.0 eV [2,6]. The adequate band gap values of both semiconductor materials are suitable for the conversion of incident solar energy from the visible spectrum. Therefore, these are considered as promising materials to be used in PEC as photocathodes and photoanodes, respectively.

In this context, a quasi onedimensional array (Q1D) at the nanoscale will generate structures that exhibit new physical properties, such as a better crystallinity and a higher integration density with a high aspect ratio due to its geometry (size of confinement in two coordinates). That is, charge carriers move a shorter distance to reach the interface [7]. So, the recombination probability decreases thereby increasing the efficiency of the SC. Therefore, in recent years, experimental techniques have been improved, which has allowed greater control of synthesis conditions [8]. Among them, highlights sonoelectrochemistry that is a technique that combines ultrasonic irradiation with electrochemical methods and has proven to be a convenient way to manipulate the size and shape of nanostructured materials [1,2,9,10]. In this way, in recent decades it has been used for the synthesis of various inorganic nanomaterials [11-14].

Thus, these nanomaterials are being applied in photoelectrochemical devices. One of these cases is the manufacture of nanostructures for energy storage and fuels production with a high relation between produced energy / CO_2 emissions. An example of the latter is hydrogen production from water splitting (eq. 1).

$$H_2O \rightarrow 1/2\,O_2 + H_2 \qquad (1)$$

This process correspond to non-spontaneous reaction which it requires 1.23 eV/e [6,15,16]. This last is also the standard potential value for the reaction. However, in order to carry out the water electrolysis, using platinum electrodes and to obtain an appreciable gas evolution, at least a potential bias between 1.4 to 1.8 V is required. This potential difference can be reduced employing electrodes based in semiconductors material where part of the energy required for eq. 1 can be obtained from the solar energy.

In this context, the metallic oxides semiconductors such as iron (III) oxide (n-Fe_2O_3) and copper (I) oxide (p-Cu_2O) appear as good candidates. Therefore, the main objective of the present work was to synthesize sonoelectrochemically, nanostructures of p-Cu_2O and nanotubes of n-Fe_2O_3 for use as photocathode and photoanode, respectively. In order to, evaluate a photoelectrochemical cell for the generation of hydrogen from the splitting of water in an alkaline solution at pH 10.

2. EXPERIMENTAL SECTION

2.1 Synthesis

In this work, the synthesis of p-Cu_2O and n-Fe_2O_3 were prepared by ultrasound-assisted anodization of copper foils (Advent Research Materials, 99.9%, 0.25 mm) and iron foil (Advent Research Materials, 99.9%, 0.25 mm), respectively. The experimental conditions for Cu_2O were: 75 V, 75°C and 900 s of polarization in a solution of ethylene glycol (EG, 99.8%, anhydrous) with 5% wt of water and 0.5% wt of NH_4Cl [1]. On the other hand, nanotubes of n-Fe_2O_3 were formed at 50 V, 50 ° C and 180 s polarization in a solution of ethylene glycol containing 3% wt of water and 0.5% wt of NH_4F [2]. The above process was carried out using a two electrode system: flag shaped 1.0 cm^2 Cu foil as anode and carbon plate, 22.55 cm^2 as cathode; the distance between cathode and anode was kept at 3 cm. The anodized samples are properly washed with distilled water and dried with Argon flow. Subsequently, the sheets were thermally treated at 190°C for 90 min in an argon atmosphere for p-Cu_2O and at 500°C for 180 min in an oxygen atmosphere for n-Fe_2O_3.

2.2 Characterization

The optical bandgap (E_g) value of Cu_2O nanostructured and nanotubes of Fe_2O_3 were determined using Kubelka-Munk equation from diffuse reflectance measurement (DRS) developed in a SHIMADZU UV-2600, the spectra were recorded between 800 and 300 nm, in air and at room temperature. The Mott Schottky plots were realized with a ZAHNER, model IM6e, potentiostat/galvanostat equipped with Thales software. For linear sweep voltammetry (LSV) measurements, an AUTOLAB PGSTAT302 potentiostat/galvanostat was used. In all cases, a conventional three-electrode electrochemical cell was employed. A platinum wire and a saturated mercury sulfate electrode (SMSE, +0.650 vs. HNE) were employed as auxiliary and reference electrodes, respectively. Electrolyte solution contained 0.1 M Na_2SO_4 pH 10, the pH value was adjusted with a 1.0 M NaOH solution and a potential sweep rate of 5 mVs^{-1}. In this work, white light was used for the experiences under illumination. For this, a 1000 W Hg: Xe 6295 ORIEL INSTRUMENTS lamp (0.5 sun) was employed.

To carry out the photoelectrolysis process of the water a cronoamperometric measurement was realized. A Teflon cell with two compartments was used, each with optical passages (Fig. 1). Both photoelectrodes were illuminated with a lamp of 0.5 soles and connected to a power source to impose a bias potential of 0.36 V. The electrochemical cells studied were: Fe|n-Fe_2O_3 nanotubes|0.1 M Na_2SO_4 (pH 10)|p-Cu_2O nanostructures|Cu.

Figure 1. Photoelectrochemical cell used in the water electrolysis experiments, with photoelectrodes of n-Fe_2O_3 and p-Cu_2O

3. RESULTS AND DISCUSSION

The oxides were grown in experimental conditions previously reported [1,2]. In the present study, the band gap (E_g) value was initially determined as a means of characterization. The E_g value of n-F_2O_3 nanotubes (2.21 eV) has been previously reported [2]. On the other hand, the E_g value corresponding to nanostructured p-Cu_2O (2.27 eV) was determined by DRS measurements (Fig. 2a). In both cases, it corresponded to a direct transition and the results obtained are concordant with those reported by other authors [17-20]. The slight increase in band gap values compared to those reported for the respective bulk phases, is associate to the decrease in the crystallite size due to quantum confinement effect. This generates an increase in the energy difference between the valence and conduction bands (band gap). [21-23].

In order to determine the semiconductor parameters of synthesized oxides, the variation of the interfacial capacitance was obtained from the Mott-Schottky plots recorded in darkness at high frequency (10 kHz) in unstirred solution at pH 10 (0.10 M Na_2SO_4) and inert atmosphere. The capacitance variation with potential was recorded in the potential range from +0.25 V to –0.40 V and –0.75 V to –1.25 V for the nanostructured p-Cu_2O and n-Fe_2O_3 nanotubes, respectively. For these measures, a Faraday cage and Pt tip connected to the reference electrode by 10 mF capacitor were employed in order to reduce the noise and error of the measurements at high frequencies.

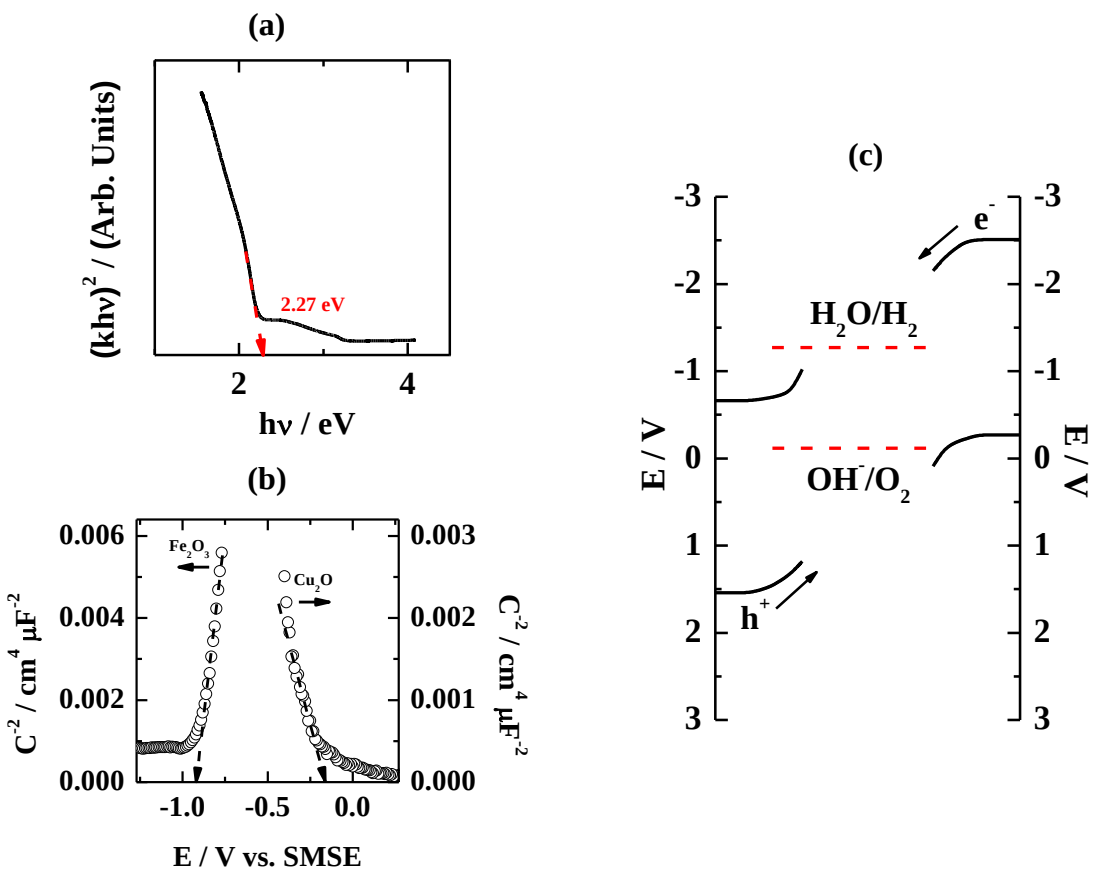

Figure 2. (a) Band gap value from diffuse reflectance measurements, (b) Mott–Schottky plots measured at 10 kHz for p-Cu_2O and n-Fe_2O_3 nanostructured electrodes in unstirred solution at pH 10 (0.10 M Na_2SO_4), in the absence of light and inert atmosphere and (c) Energy band diagram of the photoelectrochemical cell (Fe|n-Fe_2O_3 nanotubes|0.10 M Na_2SO_4 pH 10|p-Cu_2O nanostructures|Cu).

Figure 2b shows a negative slope indicating the p-type electrical conductivity of Cu_2O nanostructures [1,24] and a positive slope indicating the n-type electrical conductivity of Fe_2O3 nanotubes [2,25]. An apparent carrier majority density (N_A) of 1.62 x 10^{19} cm^{-3} and (N_D) of 11.85 x 10^{20} cm^{-3} were determined from the slope of the plot of Fig. 2b (assuming 6.3 and 80 as the dielectric constant of Cu_2O [26] and Fe_2O_3 [25], respectively) have been obtained. From the extrapolation of the straight line to $1/C^2 = 0$, flat band potential of E_{FB} = -0.15 V for Cu_2O and E_{FB} = -0.91V for Fe_2O_3 can be found.

Furthermore, from the semiconductor parameters (E_{FB} and N_A or N_D) and optical one (E_g) previously obtained, the energy bands diagrams have been constructed (see Fig. 2c). Figure shows how the bands curve because the values of the Fermi potential of the semiconductors are equal to the value of formal potential of the process to which they favor. Moreover, the photocathode (Cu_2O) curves its bands so that the Fermi level equals the formal water reduction potential at pH 10, while the valence and conduction bands of the iron (III) oxide it curves for that the Fermi level equals the formal oxidation potential of the hydroxide ion at pH 10.

From these results, the linear sweep voltammetry was recorded separately for nanostructured p-Cu_2O and n-Fe_2O_3 nanotubes. In both cases, the measures were made in a conventional cell with three electrodes in a 0.1 M Na_2SO_4 pH 10 solutions, at room temperature, with illumination and at a potential scan rate of 5 mVs^{-1} (see Fig. 3a).

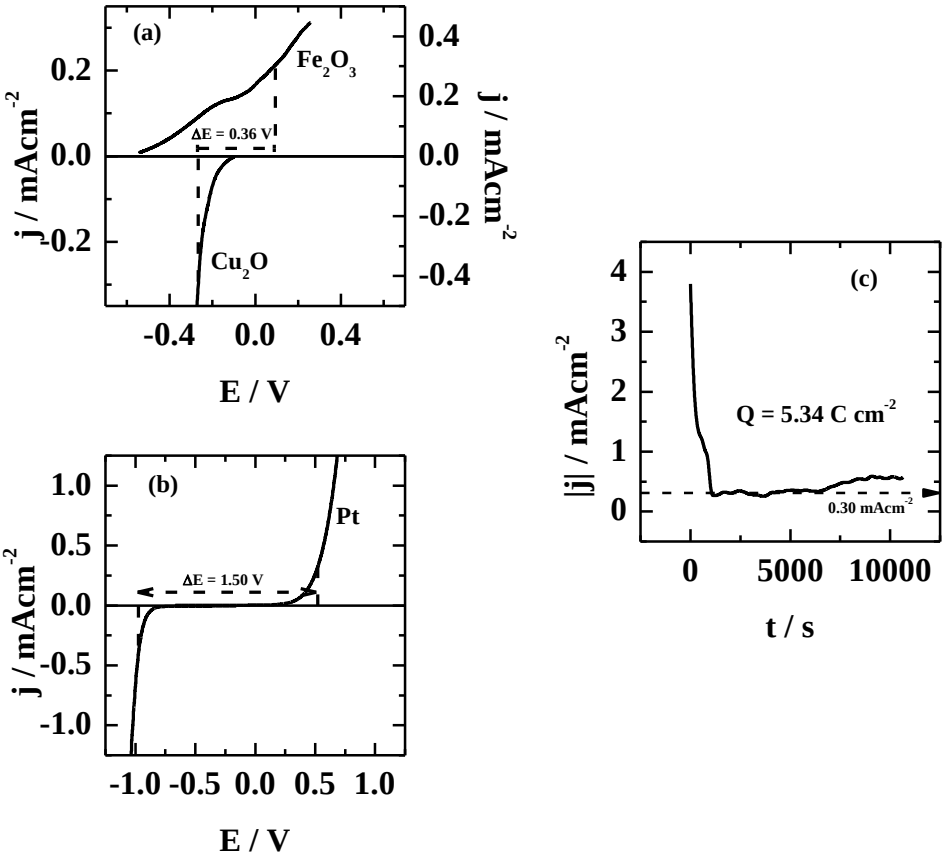

Figure 3. Linear sweep voltammetry (LSV) of (a) n-Fe_2O_3 and p-Cu_2O, both photoelectrodes under illumination conditions, (b) Pt. In (a) and (b) the experimental conditions were 0.10 M Na_2SO_4 pH 10, in an inert atmosphere and at a potential scan rate of 5 mVs^{-1}. (c) chronoamperometric curve of cell (a) with a bias potential of 0.36 V.

From figure 3a, it was possible to infer that splitting of water is spontaneous in the considered cell when both photoelectrodes are under illumination. However, it generates only 0.1 $mAcm^{-2}$ of current density. On the other hand, if the proposed photoelectrochemical cell had a potential difference of approximately 0.36 V (69.4 kJ/mol), the current density increased to almost 0.3 mA cm^{-2}. The latter showed that an amount of energy lower than that required by a cell of Pt|0.1 M Na_2SO_4 pH 10|Pt was required (Fig. 3b), which required a potential difference of approximately 1.50 V (289.5 kJ/mol) for a similar value of current density (0.3 $mAcm^{-2}$) corresponding to a decrease in 1.14 V (220.0 kJ/mol).

Fig. 3c. shows the j/t transient of the water electrolysis process for the fabricated photoelectrochemical cell, Fe|n-Fe_2O_3 nanotubes|0.1 M Na_2SO_4 (pH 10) |p-Cu_2O nanostructures|Cu, with a potential value of 0.36 V and under illumination of both photoelectrodes. The area under the curve was integrated, in order to obtain the total charge (Q = 5.34 C) involved in the electrolysis of

water. Through Faraday's law, we can calculate the amount of 0.028 mmol H_2 (6.5 x 10^{-4} L) produced in the process, assuming 100% current efficiency.

The discussion of the results obtained in the present work, show the improvements produced due to the use, in the PEC, of photoelectrodes (anode and cathode) in comparison to published results where only one photoelectrode is employed. In this context and in the study of the oxygen evolution reaction, Sima *et al.* [6] obtained photocurrent densities in a range between 0.15 to 0.5 $mAcm^{-2}$ to 1.23 V (vs. RHE) using different samples of n-Fe_2O_3 as a photoanode, when they were illuminated with sunlight (AM 1.5, 100 $mWcm^{-2}$). On the other hand, Qiu *et al.* [27] used Fe_2O_3 nanorods as a photoanode and illuminated with a 100 $mWcm^{-2}$ solar simulator (AM1.5G). The results obtained were a photocurrent density of 1.036 $mAcm^{-2}$ at 1.23 V (vs. RHE) and 800°C. Similarly, Kant *et al.* [28] obtained a maximum current density of 500 μAcm^{-2} (at 0.5 V vs. SCE) using α- Fe_2O_3/Au/ZnO as photoanode. The measurements were made in a 0.5 M NaOH solution and under AM 1.5 G illumination.

On the other hand, the use of Cu_2O as a photocatode has been reported by Jin *et al.* [29] in this work, they use Cu mesh/Cu_2O as a photocathode which exhibited a photocurrent value of 4.8 $mAcm^{-2}$ at 0 V vs. RHE under AM 1.5G lighting using a solar simulator. Similar results were reported by Shi *et al.* [30] with a photocatalyst of Cu_2O nanowires covered with a thin film of amorphous carbon. Recently, results have been reported of photocathodes that contain Cu_2O in their design. However, they present greater complexity in their synthesis [31,32].

4. CONCLUSIONS

Based on the findings of this work it is possible to establish that the methodology used to manufacture Cu_2O and Fe_2O_3 nanostructures is a low cost and clean technique. Thus, it was possible to synthesize photoelectrodes that proved to be good candidates to be used as electrodes in a photoelectrochemical cell.

From the use of the designed cell Fe|n-Fe_2O_3 nanotubes|0.1 M Na_2SO_4 (pH 10) |p-Cu_2O nanostructures|Cu, good results were obtained for the oxygen evolution reaction and for hydrogen evolution reaction from the electrolysis of water. The values were a photocurrent density of 0.3 mA $cm^{-2}$for an imposed potential of 0.36 V, decreasing in energy cost by 1.14 V, compared to the normal water electrolysis process where platinum electrodes are used.

However, there are still challenges to improve. In this regard, carry out studies to increase the stability of the Cu_2O nanostructures used in the present work.

ACKNOWLEDGEMENTS
The financial support of Fondecyt-Chile (Projects N°1140963 and N°1160485) and DI-PUCV (Projects N°125.789/2014 and 125.725/2018) is gratefully acknowledged by the authors.

References

1. P. Grez, C. Rojas, I. Segura, C. Heyser, L. Ballesteros, C. Celedón, and R. Schrebler, *Int. J. Electrochem. Sci.*, 12 (2017) 7240.

2. R. Schrebler, L.A. Ballesteros, H. Gómez, P. Grez, R. Córdova, E. Muñoz, R. Schrebler, J.R. Ramos-Barrado, and E.A. Dalchiele, *J. Electrochem. Soc.*, 161 (2014) H903.
3. Wenzhe Niu, Thomas Moehl, Wei Cui, René Wick-Joliat, Liping Zhu, and S. David Tilley, *Adv. Energy Mater.*, 8 (2018) 1702323.
4. A. Wouter Maijenburg, Michel G.C. Zoontjes, GuidoMul, *Electrochim. Acta*, 245 (2017) 259.
5. Quan-Bao Ma, Jan P. Hofmann, Anton Litke, Emiel J.M. Hensen, *Sol. Energy Mater. Sol. Cells*, 141 (2015) 178.
6. M. Sima, E. Vasile, A. Sima, *Thin Solid Films*, 658 (2018) 7.
7. T. Zhang, Z.U. Rahman, N. Wei, Y. Liu, J. Liang, and D. Wang, *Nano. Res.*, 10 (2017) 1021.
8. W. Siripala and J.R.P. Jayakody, *Sol. Energ. Mater.*, 14 (1986) 23.
9. Brett, C., Sonoelectrochemistry (Book Chapter), Piezoelectric Transducers and Applications, Springer Berlin Heidelberg, (2008) Valencia, España
10. S.K. Mohapatra, M. Misra, V.K. Mahajan, K.S. Raja, *J. Catal.*, 246 (2007) 362.
11. N. Arul Dhas, C. Paul Raj, A. Gedanken, *Chem. Mater.*, 10 (1998) 1446.
12. Xiaojun Tao, Lei Sun, Yanbao Zhao, *Mater. Chem. Phys.*, 125 (2011) 219.
13. S.K. Mohapatra, M. Misra, V.K. Mahajan, K.S. Raja, *Mater. Lett.*, 62 (2008) 1772.
14. P. Sakkas, O. Schneider, S. Martens, P. Thanou, G. Sourkouni, Chr. Argirusis, *J. Appl. Electrochem.*, 42 (2012) 763.
15. Michael G. Walter, Emily L. Warren, James R. McKone, Shannon W. Boettcher, Qixi Mi, Elizabeth A. Santori, and Nathan S. Lewis, *Chem. Rev.*, 110 (2010) 6446.
16. Allen J. Bard and Marye Anne Fox, *Acc. Chem. Res.*, 28 (1995) 141.
17. G. Li, Y. Huang, Q. Fan, M. Zhang, Q. Lan, X. Fan, Z. Zhou, C. Zhang, *Ionics*, 22 (2016) 2213.
18. B. Rajesh Kumara, B. Hymavathib, T. Subba Rao, *Mater. Today*, 4 (2017) 3903.
19. Damon A. Wheeler, Gongming Wang, Yichuan Ling, Yat Li and Jin Z. Zhang, *Energy Environ. Sci.*, 5 (2012) 6682.
20. Tapiwa Mushove, Tanya M Breault, and Levi Thompson, *Ind. Eng. Chem. Res.*, 54 (2015) 4285.
21. Freddy T. Rabouw, Celso de Mello Donega, *Top Curr. Chem. (Z)*, 374 (2016) 58.
22. Kentaro Takai, Minoru Ikeda, Takahiro Yamasaki and Chioko Kaneta, *J. Phys. Commun.*, 1 (2017) 045010.
23. Emil Roduner, *Chem. Soc. Rev.*, 35 (2006) 583.
24. P. Grez, F. Herrera, G. Riveros, R. Henríquez, A. Ramírez, E. Muñoz, E.A. Dalchiele, C. Celedón, R. Schrebler, *Mater. Lett.*, 92, 413 (2013).
25. G. Riveros, D. Ramírez, E. A. Dalchiele, R. Marotti, P. Grez, F. Martín, and J. R. Ramos-Barrado, *J. Electrochem. Soc.*, 161 (2014) D353.
26. S. Wu, Z. Yin, Q. He, X. Huang, X. Zhou, and H. Zhang, *J. Phys. Chem. C*, 114 (2010) 11816.
27. Ping Qiu, Hongfei Yang, Lianjie Yang, Qiuhe Wang, Lei Ge, *Electrochim. Acta*, 266 (2018) 431.
28. Rich Kant, Sandeep Pathak, Viresh Dutta, *Sol. Energy Mater. Sol. Cells*, 178 (2018) 38.
29. Zexun Jin, Zhuofeng Hu, Jimmy C. Yu and Jianfang Wang, *J. Mater. Chem. A*, 4 (2016) 13736.
30. Weina Shi, Xiaofan Zhang, Shaohui Li, Bingyan Zhang, Mingkui Wang, Yan Shen, *Appl. Surf. Sci.*, 358 (2015) 404.
31. Niu, W., Moehl, T., Cui, W., Wick-Joliat, R., Zhu, L., Tilley, S.D., *Adv. Energy Mater.*, 8 (2018) 1702323.
32. Xintian Xu Yizhe Liu Yuanzhi Zhu Xiaobin Fan Yang Li Fengbao Zhang Guoliang Zhang Dr. Wenchao Peng, *ChemElectroChem.*, 4 (2017) 1498.

© 2019 The Authors. Published by ESG (www.electrochemsci.org). This article is an open access article distributed under the terms and conditions of the Creative Commons Attribution license (http://creativecommons.org/licenses/by/4.0/).